Clim. Past Discuss., 7, 3541–3575, 2011
www.clim-past-discuss.net/7/3541/2011/
doi:10.5194/cpd-7-3541-2011

Climate of the Past Discussions

Multi-century tree-ring based reconstruction of the Neuquén River streamflow, northern Patagonia, Argentina

I. A. Mundo[1,2], M. H. Masiokas[1], R. Villalba[1], M. S. Morales[1], R. Neukom[3], C. Le Quesne[4], R. B. Urrutia[4,5], and A. Lara[4]

[1]Departamento de Dendrocronología e Historia Ambiental, IANIGLA, CCT CONICET Mendoza, Mendoza, Argentina
[2]LISEA, Facultad de Ciencias Agrarias y Forestales, Universidad Nacional de La Plata, La Plata, Argentina
[3]School of Earth Sciences, University of Melbourne, Melbourne, Australia
[4]Laboratorio de Dendrocronología, Instituto de Silvicultura, Facultad de Ciencias Forestales y Recursos Naturales, Universidad Austral de Chile, Valdivia, Chile
[5]Environmental Change Institute, School of Geography and the Environment, University of Oxford, Oxford, UK

Received: 6 October 2011 – Accepted: 12 October 2011 – Published: 21 October 2011

Correspondence to: I. A. Mundo (iamundo@mendoza-conicet.gob.ar)

Published by Copernicus Publications on behalf of the European Geosciences Union.

Abstract

In most cases, gauged river flow records in southern South America exist for only a few decades, hampering the detection of long-term, decadal to centennial-scale cycles and trends. Long streamflow series can be reconstructed from tree-ring records, offering the opportunity of extending the limited hydrological instrumental data for several centuries or millennia. In northern Patagonia, Argentina, the Neuquén River has great importance for local and national socio-economic activities such as hydroelectric power generation, agriculture and tourism. In this study, new and updated tree-ring chronologies from *Araucaria araucana* and *Austrocedrus chilensis* are used to reconstruct the October–June mean streamflow for the Neuquén River and place the period of gauged flows, 1903–2009, in a long-term, multi-century context. The reconstruction covers the period 1346–2000 AD and was developed through a nested principal components regression approach using a network of 43 tree-ring chronologies grouped in composite series. Analyses of the frequency, intensity, and duration of droughts and pluvial events indicate that the 20th century contains some of the driest and wettest annual to decadal-scale events in the past millennium, but longer and more severe events can also be observed in previous centuries. Blackman-Tukey and Singular Spectral Analyses identified various multi-decadal quasiperiodic oscillations with a dominant 6.8-year cycle explaining ca. 23.6 % of the total variance in the Neuquén River streamflow reconstruction. We also found that the Neuquén River discharges are related to variations in the Southern Annular Mode (SAM), a measure of air mass exchanges between middle and high latitudes in the Southern Hemisphere. This association is consistent with previous studies which indicate a strong connection between rainfall patterns in northern Patagonia and SAM activity.

1 Introduction

Water resource management requires knowledge of the natural variability in streamflow over multiple time scales (Woodhouse and Lukas, 2006). In most cases, gauged river flow records in southern South America are only a few decades long, and only a few records cover more than 100 years. Although such relatively short records are conventionally used as a basis for planning and engineering design, they are likely too short to properly determine the true flow frequency or the return period, severity, and duration of dry and wet events. Long-term trends and decadal to centennial-scale cycles are also difficult to estimate with such short time series, but they can be detected using long streamflow series reconstructed from tree-ring records (Stockton, 1975; Cook and Jacoby, 1983; Case and MacDonald, 2003; Woodhouse et al., 2006; Lara et al., 2008). By further examining the frequency (events per time period), intensity (departures from the median), and duration of events (consecutive years below or above the long-term median) in the proxy records, water resource managers may integrate reconstructed streamflow into infrastructure planning and management decisions.

The Neuquén River is one of the main rivers in the north Patagonian Andes of Argentina and drains an extensive area between 36° S and 39° S (Fig. 1). This river is used to generate hydroelectricity at the Cerros Colorados Hydropower Complex (the Planicie Banderita plant has 479 MW of installed capacity). Two large reservoirs (Los Barreales and Mari Menuco) have made extensive irrigated agriculture possible in the region. The Neuquén River has a continuous gauging station record beginning in April 1903 which is free of human interventions such as the above mentioned dams. This record represents one of the longest and best quality series in southern South America.

A preliminary dendrochronological study extended the flow series of the Neuquén and Limay Rivers back to 1601 AD (Holmes et al., 1979). This work used seven tree-ring chronologies (five from *Araucaria araucana* and two from *Austrocedrus chilensis*) available at that time. Recently, the *A. araucana* tree-ring network has been updated and expanded, encompassing 17 well-replicated chronologies that cover the period 1140–2006 AD (Mundo et al., 2011). In addition, the *A. chilensis* tree-ring network has increased to a total of 39 chronologies, including the 1800-yr long tree-ring chronology from Huinganco in the northwestern corner of the Neuquén Province (Villalba and Veblen, 1997; Morales and Boninsegna, 2000; Le Quesne et al., 2006, 2009; Christie et al., 2010). This greatly improved tree-ring network, in combination with new techniques for chronology development and climate reconstruction, provide renewed interest to improve and extend back in time the existing streamflow reconstruction for the Neuquén River with higher statistical confidence.

In this study we develop a multi-century tree-ring based reconstruction for the Neuquén River streamflow using a nested principal components regression approach. We analyze the temporal variations in water discharge and put recent streamflow variations and trends in the context of the last millennium. To facilitate the use of the reconstruction for water resource management, we also analyze the frequency, intensity, and duration of drought and pluvial events in the reconstruction and compare the reconstructed values to those observed during the instrumental period. Finally, in order to identify the major climatic forcings influencing river discharge, we compare the Neuquén River reconstruction with hemispheric or global atmospheric circulation indexes.

2 Data and methods

2.1 Streamflow data

The Neuquén River basin covers 49 958 km^2 including mainly the northern part of the Neuquén Province and a small northwestern portion of the Río Negro Province in northwestern Patagonia, Argentina (Fig. 1). As mentioned above, this river is regulated by the Cerros Colorados Complex which consists of four dams (Portezuelo Grande, Loma de la Lata, Planicie Banderita and El Chañar). Their primary purposes are to control

CPD
7, 3541–3575, 2011

surge, regulate flows and ensure water supply for human consumption, irrigation, and hydroelectric generation.

The hydrological year for the Neuquén streamflow is usually considered from April to March (Fig. 2). The hydrograph is characterized by a bimodal regime: the first peak occurs in winter associated with cold season precipitation in the basin, and the second peak in late spring largely due to snow melt. The Subsecretaría de Recursos Hídricos de la Nación (SSRH, the National Agency of Water Resources of Argentina) has eight gauges throughout the Neuquén basin. The Paso de Indios record (38°31′55″ S; 69°24′49″ W; 498 m a.s.l.; Fig. 1) is one of the longest records available in southern South America (1903–2011). The average flow of the Neuquén River at Paso de Indios is 312 $m^3 s^{-1}$, but maximum flows of up to 10 350 $m^3 s^{-1}$ were recorded on 13 July 2006 in Portezuelo Grande dam. The average of monthly streamflow was evaluated with tree-ring data to determine the most appropriate months or seasons to develop the streamflow reconstruction.

2.2 Tree-ring network

The tree species selected to develop the Neuquén River streamflow reconstruction were the precipitation-sensitive, evergreen conifers *Araucaria araucana* and *Austrocedrus chilensis. A. araucana* extends from ca. 37°20′ to 40°20′ S in the Andes of southwestern Argentina and southcentral Chile (Veblen, 1982). This species occurs from elevations as low as 600 m (especially on the Argentinean side of the Andes) to ca. 1800 m and 1500 m in the northern and southern timberlines along its distribution range, respectively. Annual precipitation in this region ranges from ca. 1200 mm on the Argentinean side of the Andes to well over 4000 mm on the west-facing slopes at ca. 39° S (Almeyda and Sáez, 1958). The climate in these areas has a Mediterranean regime with a peak of precipitation in winter and dry summers (Donoso-Zegers, 1993). The intensity and duration of summer droughts increase markedly northwards and are reflected in the species-poor and sparse understory vegetation in the northerly *Araucaria* stands. *Araucarias* of ca. 900 years of age have been recorded from marginal

CPD
7, 3541–3575, 2011

forest patches on rocky outcrops surrounded by the xeric steppe and in the northern slope of Lanín Volcano in Argentina (LaMarche et al., 1979; Mundo et al., 2011).

Austrocedrus grows mainly on the steep topography of the Andean Cordillera between 32°39′ S and 38° S on the western slopes and between 37°07′ and 43°44′ S on the eastern slopes of the Andes. The growth of *Austrocedrus* is particularly sensitive to precipitation. Individuals can live more than 1200 years (Villalba and Veblen, 1997; Le Quesne et al., 2006). Wood samples from *Austrocedrus* at El Asiento (Chile, 32°40′ S; 70°49′ W) and Huinganco (Argentina, 36°30′ S; 70°36′ W) stands have provided exceptionally long chronologies covering the past 1200 to 1800 years (Morales and Boninsegna, 2000; Le Quesne et al., 2006).

The tree-ring data considered in this study (66 individual chronologies) were obtained from unpublished collections and published chronologies freely available on the International Tree-Ring Data Bank (ITRDB)[1] (Fig. 1, Table 1 and Table 1 in the Supplement). Although many chronologies are located outside of the Neuquén River basin, they were all initially included as potential predictors of streamflows to capture the regional-scale hydroclimatic variability related to the Neuquén River discharge (Cook et al., 1999; Woodhouse and Lukas, 2006).

Tree-ring chronologies were initially standardized using a cubic spline function designed to reduce 50 % of the variance in a sine wave with a periodicity of 150 years (Cook and Peters, 1981). Varimax rotated principal components (PC) were extracted from these records for the 1800–1950 AD common period that coincides with the interval of higher replication of site chronologies. The selection of this period assures that the signal in each record is representative of the stand growth, reducing the noise associated with low series replication in the chronologies. For each species, all records contributing to a PC with factor loadings >0.60 were combined to develop regional composite chronologies (Fig. 1 in the Supplement). The factor loadings of each chronology

[1]The International Tree-Ring Data Bank (ITRDB) held at the World Data Center for Paleoclimatology website (NOAA Paleoclimatology Program, http://www.ncdc.noaa.gov/paleo/treering.html).

to the corresponding PC are listed in Table 1 in the Supplement. All tree-ring series shorter than 100 years were excluded from the regional composite chronologies. In the development of these composite records, all ring width series were standardized using the computer program ARSTAN (Cook, 1985). Standardization was accomplished by fitting a negative exponential curve or straight line with any slope to each individual ring width series. The variance of the resulting chronologies was adjusted to account for changes in sample size backward in time (Osborn et al., 1997). The ARSTAN chronologies (Cook, 1985) were used in the analyses discussed in this paper.

The quality of the chronologies was assessed on the basis of the following statistics: mean sensitivity (MS), the average correlation between all series (RBAR), the expressed population signal (EPS) and the first-order autocorrelation of the series. Mean sensitivity represents a measure of the interannual variability in tree rings (Fritts, 1976), whereas the RBAR is a measure of the common variance between all series in a chronology (Wigley et al., 1984). Running RBAR illustrates changes in the strength of common patterns of tree growth over time. EPS measures how well the finite-sample chronology compares with a theoretical population chronology based on an infinite number of trees (Wigley et al., 1984). The RBAR and EPS values were computed using a 50-year moving window with a 25-year overlap. We used the EPS cutoff point of 0.85, suggested by Wigley et al. (1984), to identify the period with reasonable signal strength in each chronology (Table 1, Fig. 2 in the Supplement).

2.3 Reconstruction method

To identify the relationships between streamflow and tree growth, we computed correlations coefficients between tree-ring width indices from the composite chronologies and monthly mean Neuquén River streamflow records (Fritts, 1976; Blasing et al., 1984). The highest correlation was generally found between tree-ring composite chronologies and the mean seasonal flows from October to June (9-month period). This mean 9-month streamflow series shows no significant departure from normality (Shapiro-Wilk $W = 0.987$; $p = 0.421$).

CPD
7, 3541–3575, 2011

A nested principal component regression (PCR) approach, which accounts for the decrease in the number of predictor chronologies backward in time, was chosen to reconstruct mean October–June Neuquén River streamflow (Meko, 1997; Cook et al., 1999, 2002). All composite ARSTAN chronologies were initially lagged ($t = 0$, $t - 1$, $t + 1$, and $t + 2$) to capture possible climate-related persistence in the tree-ring series (Fritts, 1976). The overlap period between the instrumental streamflow record and the tree ring chronologies (1903–2000) was split into two periods, using the interval 1951–2000 for calibration and reserving the interval 1903–1950 for verification of the model. Then, we reversed the process and tested the model selecting the earliest years (1903–1950) for calibration and withholding the latest years (1951-2000) for verification. A principal components analysis (PCA) was calculated on the pool of series significantly correlated ($p < 0.05$) with mean October–June streamflow during the calibration period. Following the Kaiser-Guttman rule, the eigenvectors with eigenvalues >1 were retained for the multiple regression, further reducing the dimensionality of the dataset. The final subset of principal components in the regression model was determined using the minimum AIC that includes a penalty term for increasing the number of predictors in the model (Akaike, 1974). The model skill was evaluated using the reduction of error (RE), the coefficient of efficiency (CE), and the sign test statistics, three tests of fitness commonly used in dendrochronology (Fritts, 1976; Cook et al., 1999). We applied this technique to develop six reconstruction models based on different sets of increasingly longer tree-ring composite series, in which the shortest series were excluded one at a time. The models were finally calibrated over the complete 1903–2000 overlapping period and used to reconstruct the predictand series over the full length of the composite tree-ring series. To derive the final reconstruction we selected the models that showed the best calibration and verification statistics and spliced together their corresponding reconstructed series. The mean and variance of each reconstructed series were adjusted (normalized) to that of the most replicated nest in order to minimize artifact-related changes in variance through time.

CPD
7, 3541–3575, 2011

The relative influence of each predictor (composite chronology) on the final reconstruction during the common nest period was evaluated by considering the absolute value of the standardized regression coefficients or beta weights (Cook et al., 1999, 2002). The beta weights represent the principal component loadings of the predictor chronologies in the model and are calculated by multiplying the matrix of retained eigenvectors by the vector of beta weights in the principal component space (Cook et al., 1994). We summed the absolute beta weights for composite chronologies where the t, $t-1$, $t+1$ and $t+2$ series were included as predictors, and then divided by the total sum of the beta weights for all predictors in the complete calibration model to calculate a measure of relative variance explained (0–100 %) for each composite (Frank and Esper, 2005).

Intensity and duration of events (droughts or pluvials) in the Neuquén River streamflow were examined by computing the 5 lowest and highest reconstructed n year running means for $n = 1$, 5, 11, and 25 years. The most severe n year events from the instrumental period were calculated for comparison to the reconstructed record of streamflow. The frequency domains of the instrumentally recorded and reconstructed streamflow variations in the Neuquén River were assessed using power-spectral and coherency analyses (Jenkins and Watts, 1968). The Blackman-Tukey (BT) spectra were computed over the period 1903–2000, common to both the actual and reconstructed records. Twenty lags (20 % of the series length) of the auto- and cross-covariance functions were employed and smoothed with the Hamming filter. The 95 % confidence level of the spectrum was estimated from a "red noise" first-order Markov null continuum based on the lag-1 autocorrelation of the time series (Mitchell et al., 1966). We also used BT and singular spectral analyses (SSA) to establish the significant dominant periods at which variance occurs in the streamflow reconstruction. For the streamflow reconstruction, the BT spectrum was estimated from 131 lags of the autocorrelation function. With this number of lags (20 % of the series length), we set a reasonable balance between high resolution and moderate stability. SSA is basically a statistical technique related to empirical orthogonal function analysis to determine

CPD
7, 3541–3575, 2011

oscillatory modes in the time space. Quasiperiodic signals appear as pairs of degenerate eigenmodes and their corresponding eigenfunctions in the time domain are orthogonal with each other (Vautard and Ghil, 1989). Similar to other spectral techniques, the choice of lags in SSA is a compromise between the amount of information to be retained (resolution) and statistical significance (stability). We experimented with lags ranging from 1 to 5 % of the series length, and we found that a lag equal to 2 % of the series length (11 years) adequately resolved most decadal-scale oscillatory modes.

In order to identify the influence of El Niño-Southern Oscillation (ENSO) and the Southern Annular Mode (SAM) on the Neuquén River streamflow, Pearson's correlation coefficients between the streamflow reconstruction, sea surface temperature for El Niño 3.4 zone (ERSST.v3B Niño 3.4), Southern Oscillation Index (SOI) (both series available at http://www.cpc.ncep.noaa.gov/data/indices/), and an extended SAM index (http://www.ifm-geomar.de/index.php?id=sam) (Visbeck, 2009) were evaluated. Correlations were assessed after removing the autocorrelation in the reconstruction, and in the ENSO and SAM time series. In this case we used an autoregressive model where the order was estimated from the Akaike information criterion AIC (Akaike, 1974). Using autocorrelated series in this analysis would make the statistical tests of correlation too liberal (i.e. too frequent rejection of the null hypothesis, $r = 0$) (Masiokas et al., 2006). Correlations using 21-year central moving windows were also calculated to assess possible changes in the strength of the relationships between the reconstruction and these two indices.

3 Results

3.1 The tree-ring network

The PCA grouped the *Araucaria* chronologies in six significant components which accounted for 40.1, 8.3, 6.4, 6.2, 4.8 and 4.3 % of the total variance, respectively. The *Austrocedrus* chronologies were also joined in six significant components accounting for 37.0, 11.8, 7.7, 5.9, 4.3 and 3.6 % of the total variance (see Table 1 in the Supplement). Based on the factor loadings, the chronologies of both species were combined in six composite chronologies (*Araucaria*: AR1, AR2, AR3, AR4, AR5 and AR6; *Austrocedrus*: AU1, AU2, AU3, AU4, AU5 and AU6). As the total number of tree-ring series in the AR4, AR5 and AR6 composite chronologies was below 50, we decided not to include them in the analyses. The number of tree-ring radii in the remaining composite chronologies ranges between 64 and 541 (Table 2).

3.2 Analysis of the reconstruction

Table 2 shows the calibration and verification statistics of the different regression models used to reconstruct the Neuquén River streamflow. Model 2 shows a slightly higher statistical skill than Model 1 and was therefore selected to estimate streamflow for the more recent period 1676–2000 AD. Models 4 and 5 also show reasonable skill in predicting streamflow and were used to extend back in time the reconstruction (back to 1487 AD with Model 4 and to 1346 AD with Model 5). The skill of the regression model that could extend further back in time the reconstructed series (Model 6, Table 2) is poor compared to the other, better replicated models. Thus, Model 6 was not included in the analyses. The final nested reconstruction based on the *Araucaria* and *Austrocedrus* composite tree-ring chronologies spans from 1346 AD to 2000 (Fig. 3). The three intervening models explain between 43.1 and 48.2 % of the total variance in the instrumental streamflow record over the common period 1903–2000 (Table 2). The *F* value of these models ranges between 21.59 and 39.27, and their calibration and verification (RE and CE) statistics remain positive for the segments 1903–1950 and 1951–2000 (Table 2). The sign test results, an indication of how well the tree-ring estimates track the direction of change in climate from year to year, were significant at or above the 0.05 level for these models. Analyses of regression residuals indicate no violations of regression assumptions. The residuals of these regression models are approximately normally distributed and not significantly autocorrelated according to Durbin-Watson tests (Fig. 3b). Model 6, based on a reduced number of predictors (AU4 and AU6), shows a lower percentage of variance accounted for by regression and RE and CE values close to zero (Table 2).

The beta weights for Model 2 are shown in Fig. 1b. Seven composite chronologies were retained for modeling, and weights were distributed across the region and species type. The mean relative variance explained for all composite chronologies was 16.7 %, ranging from 0.1 % to 27.4 %. The highest values were observed for *Austrocedrus* composite chronologies (AU1, AU4 and AU6) which grouped tree-ring chronologies from southern and northern sites of the basin.

3.3 Frequency, intensity and duration of events

The Neuquén River reconstructed record (1346–2000) shows important inter-annual to multi-decadal variability, with several transitions from dry to wet or wet to dry intervals being common throughout the reconstruction (Fig. 3c). Overall, the reconstructed record shows drought events more severe than those recorded in the instrumental record. In contrast, reconstructed pluvial events are less wet than observed. A list of the lowest and highest streamflows reconstructed for the Neuquén River since 1346 shows that three of the five lowest October–June streamflows occurred during the 20th century, with the lowest being 1968 (Table 3). In both, measurements and reconstruction, one of the driest years of the instrumental period is 1998, representing also the second driest year of the entire 1346–2000 reconstruction. In relation to the highest streamflow years, the years 1940 and 1992 were reported in this category during the 20th century. Across the streamflow reconstruction the 5-year lowest streamflow periods were 1817–1821 and 1909–1913, and the two 5-year highest streamflow periods were 1589–1593 and 1833–1837. Three of the 5-year lowest and two of the 5-year highest streamflow periods were recorded in the 20th century.

In terms of the 10-year moving averages, the period from 1908 to 1917 was ranked the driest among the five lowest streamflow events over the past 655 years, and the period from 1829 to 1838 was ranked at the top of the highest streamflows in the last

CPD
7, 3541–3575, 2011

six centuries. Longer periods with low streamflow values in the reconstruction were 1802–1826, 1889–1913, 1952–1976, 1765–1789, and 1677–1701 (Fig. 3c).

3.4 Spectral analyses

Results from a coherence spectral analysis between the observed and reconstructed streamflows over the common period 1903–2000 revealed congruence at interannual, decadal, and interdecadal time scales with significant squared coherency at around 2.5–3.3, 10, 13, 20 and 40 year cycles (Fig. 4b). These bandwidths contain the largest proportion of the reconstructed variance.

The Blackman-Tukey spectrum of the reconstructed Neuquén River streamflow over the period 1346–2000 show peaks that exceed the 95 % confidence limit at 17.5, 6.6, 5.2 and 3.4 years (Fig. 5). Six major waveforms, representing decadal to interannual modes of common variance at 47, 17.6, 6.8, 5.1 and 3.8 years, were isolated from the streamflow reconstruction using Singular Spectral Analysis (Vautard and Ghil, 1989; Fig. 6). The temporal evolution of these components accounts for 84.4 % of the total variance in the reconstruction.

3.5 Climate influence

Variations in the Neuquén River streamflow reconstruction could not be significantly explained by ENSO variations tested using SST data in the Niño 3.4 zone and the SOI index. In contrast, correlations between the Neuquén streamflow reconstruction and annual SAM index demonstrate that the Neuquén October–June streamflow is significantly correlated with this forcing across the 1887–2000 period (Fig. 7a). However, correlations using a 21-year central moving window revealed an interesting pattern with changes in the strength of these correlations over time. The reconstructed Neuquén River streamflow was significantly correlated with SAM at the end of 19th century–beginning of 20th century (between 1897–1920) and at mid (1943–1958) and end of the 20th century (Fig. 7b).

CPD
7, 3541–3575, 2011

Spatial correlations between the instrumental and reconstructed October–June Neuquén River streamflow and the geopotential heights (500 HPa) were estimated for the area 20° N–85° S/180° E–0° (Fig. 8). Both streamflow series show similar correlation patterns with the geopotential heights. Consistent with the SAM relationship previously described, October–June Neuquén River streamflow is positive and significantly correlated with geopotential heights over Antarctica during the October–June period.

4 Discussion

In this paper we present a tree-ring based reconstruction of mean October–June Neuquén River streamflow which complement and extend the pioneering reconstruction of Holmes et al. (1979) developed for the 1601–1968 period. This new series extends back in time the Neuquén River streamflow by 290 years, substantially increases the number of tree-ring chronologies used as predictors and uses newer methods for capturing the mean and variance of the instrumental record over a significantly longer calibration period. To our knowledge, the Neuquén River reconstruction represents the longest streamflow reconstruction in South America.

The *Araucaria araucana* and *Austrocedrus chilensis* composite chronologies used in this study are robust, well-replicated proxy records. The descriptive statistics of the composite chronologies are comparable to those previously reported for both species (Villalba et al., 1998; Mundo et al., 2011). During the 1676–2000 period, the greatest contribution to the streamflow (41.0 %), expressed as percentage of beta weigths, was provided by the AU6 composite which grouped two chronologies (Melado and Huinganco) at the northern limit of the basin (35°52′S–37°07′ S). However, the 50.1 % of contribution to the streamflow reconstruction, was provided additively by AU1 and AU4, composite series which grouped chronologies located in the south (39°15′ S–41°10′ S) and north (32°39′ S–34°46′ S) of the study area. The significant correlation between these chronologies with the Neuquén River streamflow suggests that the precipitation regime in the Neuquén watershed represents a transitional pattern between the central Chile and the northern Patagonia precipitation regimes. This situation was also recorded for the Maule watershed located at 35° S–36°30′ S on the Chilean slope of the Andes (Urrutia et al., 2011).

The final nested reconstruction models explain 43.1 and 48.2 % of the total variance in the October–June Neuquén River streamflow over the 1903–2000 calibration period. This range of values is similar to those reported for the streamflow reconstructions of the binational Puelo River (Lara et al., 2008) and the Chilean Maule River (Urrutia et al., 2011) in the western side of the north Patagonian Andes. The total variance explained by our model is lower than that recorded in the previous reconstruction of the annual Neuquén River streamflow developed by Holmes et al. (1979; 53.3 % of explained variance). We believe that the use of highly correlated chronologies as predictors in their multiple regression model may have partially inflated the percentage of variance accounted for by the regression equation.

The 20th century has seen some of the driest and wettest annual to decadal events in the past millennium, but longer and more severe events were reconstructed in previous centuries. Four of the five years with the lowest streamflows in the last 655 years occurred in the 20th century. The lowest reconstructed streamflow was 1968, which was also a great-intensity drought year in Mendoza province, affecting water availability for irrigation, water consumption in the city of Mendoza and electric power generation in the Atuel River (Prieto et al., 2010). The lowest observed streamflow was 1998, which was also the second lowest reconstructed streamflow. In 1998–1999, strong La Niña conditions in the western tropical Pacific and an anomalously high polarity of the Antarctic Oscillation (i.e. a strengthened polar vortex; Thompson and Wallace, 2000) led to severe drought in northern Patagonia (annual rainfall was the lowest since recordings began in 1905; Suarez et al., 2004). This climatic event resulted in massive mortality of the evergreen tree *Nothofagus dombeyi* near its eastern distributional limit towards the Patagonian steppe (Suarez et al., 2004). Additionally, during the 1998–1999 fire season more than 14 000 ha burned in the Nahuel Huapi National Park alone

CPD
7, 3541–3575, 2011

(Veblen et al., 2003). The year 1998 was also reported among the 10 driest years in the December PDSI reconstruction for the Temperate-Mediterranean transition (TMT) zone of the Andes in Chile (35.5°–39.5° S; Christie et al., 2010). The forth lowest reconstructed streamflow was 1924, which was also the year with the lowest annual precipitation recorded in Santiago de Chile (Rutllant and Fuenzalida, 1991) and the lowest reconstructed annual streamflow of Maule watershed (Urrutia et al., 2011). The three of the four lowest streamflows in the 20th century in the Neuquén River streamflow reconstruction (1908, 1924, 1968, and 1998) were also registered as part of the 10 driest years of the 800 year central Chile precipitation reconstruction (Le Quesne et al., 2006). Two of the 5-year periods with the lowest streamflows closely match with periods observed in the Puelo River and Maule River streamflow reconstructions (1908-1917 and 1812–1821). The period 1817–1821 also had a close correspondence with the low annual precipitation registered in a reconstruction for northern Patagonia (Villalba et al., 1998).

Pluvial events of the late 20th century rank among the wettest in the reconstruction, but in some cases the intensity of these events was underestimated in the model (pluvial 1914), suggesting that reconstruction was conservative in the representation of extreme wet events. This is a common feature in hydroclimatic reconstructions from tree rings (Maxwell et al., 2011). Two of the five highest reconstructed streamflow years occurred during the 20th century. The year 1940 was also reported as one with the highest flows in the streamflow reconstructions of Puelo River (Lara et al., 2008) and Maule watershed (Urrutia et al., 2011). This year was also recorded as one with the highest pluvials in the reconstruction using *Nothofagus pumilio* tree-ring chronologies in the central Andes of Chile (Lara et al., 2001).

Blackman-Tukey and Singular Spectral Analyses applied to the reconstruction indicates that the temporal variability is dominated by a 6.6–6.8-year cycle which explains approximately 23.6 % of the total variance in the Neuquén River streamflow reconstruction (Figs. 5 and 6). Similar oscillations were also found in the Puelo River streamflow reconstruction (5–6.5 years; Lara et al., 2008) and in the annual precipitation

CPD
7, 3541–3575, 2011

reconstruction for northern Patagonia (6.2–6.4 years; Villalba et al., 1998). Power spectra and Singular Spectral Analysis of the streamflow reconstruction also indicate the presence of lower-frequency oscillations at periods of approximately of 17.6 years. Oscillations on the order of 17 years have also been documented in temperature and precipitation reconstructions for northern Patagonia (Villalba et al., 1996, 1998). The shortest mode of variability in the reconstruction (3.8–3.4 years) may correspond to the El Niño–Southern Oscillation recurrence cycle. Trenberth (1975, 1976) found the quasi-biennial oscillation (QBO) to be very marked in some circulation indices of the Southern Hemisphere.

Knowledge of past drought and pluvial events is important for water resource management in the Neuquén River Basin. However, the instrumental record of Neuquén River streamflow does not adequately represent the full range of variability in the past 655 years, as evidenced by our reconstruction of streamflow. Extreme drought and pluvial events ranging from 1–25 years in duration have occurred during the period of the instrumental record, but more severe drought events were represented by the reconstruction (for example: 1802–1826, 1889–1893, 1765–1789, 1677–1701).

The Neuquén River streamflow is also related to variations in the SAM, the dominant pattern of variability in the tropospheric circulation south of 20° S (Thompson and Wallace, 2000). The positive phase of SAM is associated with a decrease in surface pressure and geopotential heights over Antarctica and a strengthening and poleward shift of the Westerlies (Garreaud et al., 2009). Opposite conditions prevail during the negative phase. During positive phases of the AAO there is a marked decrease in rainfall in northern and central Patagonia and increased precipitation during negative phases (Aravena and Luckman 2009).

This study is especially useful in understanding the temporal variability of water availability in northern Patagonia, where water is fundamental for economic activities such as hydroelectric power generation, agriculture and tourism. According to the IPCC (2007), this Andean region in northwestern Patagonia is projected to experience an important reduction in precipitation by the end of the 21st century. Detailed, quantitative information on past hydrological changes may provide base information to better prepare for these drier scenarios. Further improvements in the existing reconstructions could be achieved by expanding the temporal and spatial coverage of the tree-ring network in northern Patagonia. Similar reconstruction exercises could be performed for other Patagonian rivers of great socio-economic importance for the region such as the Colorado, Limay and Chubut. The integration of streamflow reconstructions into water management practices and infrastructure planning appears as a really challenging goal which will require significant efforts and close collaboration between dendroclimatologists, climatologists, hydrologists and regional water resource managers.

Supplementary material related to this article is available online at: http://www.clim-past-discuss.net/7/3541/2011/cpd-7-3541-2011-supplement.pdf.

Acknowledgements. This research was supported by the Inter-American Institute for Global Change Research (IAI-CRN 2047) and by a CONICET post-doctoral fellowship (National Council for Scientific and Technical Research of Argentina). We thank the Subsecretaría de Recursos Hídricos de la Nación (National Agency of Water Resources of Argentina) for providing the record of Paso de Indio gauge in Neuquén province. We also thank Petr Stepanek for providing the AnClim software which allowed the calculation of power spectra (http://www.climahom.eu).

PAGES PAST GLOBAL CHANGES The publication of this article was sponsored by PAGES.

References

Akaike, H.: A new look at the statistical model identification, IEEE T. Automat. Control AC, 19, 716–723, 1974.

Almeyda, A. E. and Sáez, S. F.: Recopilación de Datos Climáticos de Chile y Mapas Sinópticos Respectivos, Ministerio de Agricultura, Santiago de Chile, 1958.

Aravena, J. C. and Luckman, B. H.: Spatio-temporal rainfall patterns in southern South America, Int. J. Climatol., 29, 2106–2120, 2009.

Blasing, T. J., Solomon, A. M., and Duvick, D. N.: Response function revisited, Tree-Ring Bull., 44, 1–15, 1984.

Case, R. A. and MacDonald, G. M.: Tree ring reconstructions of streamflow for three Canadian Prairie rivers, J. Am. Water. Resour. Assoc., 39, 703–716, 2003.

Christie, D. A., Boninsegna, J. A., Cleaveland, M., Lara, A., Le Quesne, C., Morales, M., Mudelsee, M., Stahle, D., and Villalba, R.: Aridity changes in the Temperate-Mediterranean transition of the Andes since AD 1346 reconstructed from tree-rings, Clim. Dynam., 36, 1505–1521, doi:10.1007/s00382-009-0723-4, 2010.

Cook, E. R.: A time series analysis approach to tree ring standardization, University of Arizona, School of Renewable Natural Resources, Tucson, 1985.

Cook, E. R.: The decomposition of tree-ring series for environmental studies, Tree-Ring Bull., 47, 37–59, 1987.

Cook, E. R. and Jacoby, G. C.: Potomac River streamflow since 1730 as reconstructed by Tree Rings, J. Clim. Appl. Meteorol., 22, 1659–1672, 1983.

Cook, E. R. and Peters, K.: The smoothing spline: a new approach to standardizing forest interior tree-ring width series for dendroclimatic studies, Tree-Ring Bull., 41, 45–53, 1981.

Cook, E. R., Briffa, K., and Jones, P.: Spatial regression methods in dendroclimatology: A review and comparison of two techniques, Int. J. Climatol., 14, 379–402, 1994.

Cook, E. R., Briffa, K., Shiyatov, S., and Mazepa, V.: Tree-ring standardization and growth-trend estimation, in Methods of dendrochronology – applications in the environmental sciences, edited by: Cook, E. and Kairiukstis, L. A., Kluwer Academic Publishers, Amsterdam, 104–132, 1990.

Cook, E. R., Meko, D. M., Stahle, D. W., and Cleaveland, M. K.: Drought reconstructions for the continental United States, J. Climate, 12, 1145–1162, 1999.

CPD
7, 3541–3575, 2011

Multi-century tree-ring based reconstruction of the Neuquén River

I. A. Mundo et al.

Cook, E. R., D'Arrigo, R., and Mann, M.: A well-verified, multiproxy reconstruction of the winter North Atlantic Oscillation index since A.D. 1400, J. Climate, 15, 1754–1764, 2002.

Donoso-Zegers, C.: Bosques templados de Chile y Argentina, Editorial Universitaria, Santiago de Chile, 1993.

Frank, D. and Esper, J.: Temperature reconstructions and comparisons with instrumental data from a tree-ring network for the European Alps, Int. J. Climatol., 25, 1437–1454, 2005.

Fritts, H. C.: Tree Rings and Climate, Academic Press, London, 1976.

Garreaud, R. D., Vuille, M., Compagnucci, R., and Marengo, J.: Present-day South American climate, Palaeogeogr. Palaeocl., 281, 180–195, doi:10.1016/j.palaeo.2007.10.032, 2009.

Holmes, R. L., Stockton, C. W., and LaMarche, V. C.: Extension of river flow records in Argentina from long tree-ring chronologies, J. Am. Water. Resour. Asoc., 15, 1081–1085, 1979.

Jenkins, G. M. and Watts, D. G.: Spectral analysis and its applications, Holden-Day, San Francisco, 1968.

LaMarche, V. C., Holmes, R. L., Donwiddie, P., and Drew, L.: Tree-ring chronologies of the southern hemisphere: 1. Argentina, University of Arizona, Tucson, 1979.

Lara, A., Aravena, J. C., Villalba, R., Wolodarsky-Franke, A., Luckman, B. H., and Wilson, R.: Dendroclimatology of high-elevation *Nothofagus pumilio* forests at their northern distribution limit in the central Andes of Chile, Can. J. Forest. Res., 31, 925–936, 2001.

Lara, A., Villalba, R., and Urrutia, R. B.: A 400-year tree-ring record of the Puelo River summer–fall streamflow in the Valdivian Rainforest eco-region, Chile, Climatic Change, 86, 331–356, doi:10.1007/s10584-007-9287-7, 2008.

Le Quesne, C., Stahle, D. W., Cleaveland, M. K., Therrell, M. D., Aravena, J. C., and Barichivich, J.: Ancient *Austrocedrus* tree-ring chronologies used to reconstruct central Chile precipitation variability from a.d. 1200 to 2000, J. Climate, 19, 5731–5744, doi:10.1175/JCLI3935.1, 2006.

Le Quesne, C., Acuña, C., Boninsegna, J. A., Rivera, A., and Barichivich, J.: Long-term glacier variations in the Central Andes of Argentina and Chile, inferred from historical records and tree-ring reconstructed precipitation, Palaeogeogr. Palaeocl., 281, 334–344, doi:10.1016/j.palaeo.2008.01.039, 2009.

Masiokas, M. H., Villalba, R., Luckman, B. H., Le Quesne, C., and Aravena, J. C.: Snowpack variations in the central Andes of Argentina and Chile, 1951–2005: large-scale atmospheric influences and implications for water resources in the region, J. Climate, 19, 6334–6352, doi:doi:10.1175/JCLI3969.1, 2006.

CPD
7, 3541–3575, 2011

Maxwell, R. S., Hessl, A. E., Cook, E. R., and Pederson, N.: A multispecies tree ring reconstruction of Potomac River streamflow (950–2001), Water Resour. Res., 47, W05512, doi:10.1029/2010WR010019, 2011.

Meko, D.: Dendroclimatic reconstruction with time varying predictor subsets of tree indices, J. Climate, 10, 68-696, doi:10.1175/1520-0442(1997)010¡0687:DRWTVP¿2.0.CO;2, 1997.

Mitchell, J. M., Dzerdseevskii, B., Flohn, H., Hofmeyr, W. L., Lamb, H. H., Rao, K. N., and Wallen, C. C.: Climatic change, World Meteorological Organization, 1966.

Morales, M. S. and Boninsegna, J. A.: ENSO signal in a new long tree-line chronology from *Austrocedrus chilensis* at Huinganco, Neuquén, Argentina, in International Conference of Dendrochronology for the Third Millenium, Laboratorio de Dendrocronología, IANIGLA-CONICET, Mendoza, Argentina, p.235, 2000.

Mundo, I. A., Roig Juñent, F. A., Villalba, R., Kitzberger, T., and Barrera, M. D.: *Araucaria araucana* tree-ring chronologies in Argentina: spatial growth variations and climate influences, Trees-Struct. Funct., doi:10.1007/s00468-011-0605-3, in press, 2011.

Osborn, T. J., Briffa, K., and Jones, P. D.: Adjusting variance for sample-size in tree-ring chronologies and other regional mean time series, Dendrochronologia, 15, 89–99, 1997.

Priestley, M. B.: Spectral analysis and time series, Academic Press, London, 1992.

Prieto, M. R., Araneo, D., and Villalba, R.: The Great Droughts of 1924–25 and 1968–69 in the Argentinean Central Andes: Socio-economic impacts and responses, in: II International Symposium "Reconstructing Climate Variations in South America and the Antarctic Peninsula over the last 2000 years", CIN-Facultad de Ciencias Forestales y Recursos Naturales, UACH-PAGES, Valdivia, Chile, p.57, 2010.

Rutllant, J. and Fuenzalida, H.: Synoptic aspects of the central Chile rainfall variability associated with the Southern Oscillation, Int. J. Climatol., 11, 63–76, 1991.

Stockton, C. W.: Long-Term Streamflow Records Reconstructed From Tree-Rings, University of Arizona, Tucson, Arizona, 1975.

Suarez, M. L., Ghermandi, L., and Kitzberger, T.: Factors predisposing episodic drought-induced tree mortality in *Nothofagus*-site, climatic sensitivity and growth trends, J. Ecol., 92, 954–966, 2004.

Thompson, D. W. J. and Wallace, J. M.: Annular modes in the extratropical circulation, Part I: Month-to-month variability, J. Climate, 13, 1000–1016, 2000.

CPD
7, 3541–3575, 2011

Multi-century tree-ring based reconstruction of the Neuquén River

I. A. Mundo et al.

Trenberth, K. E.: A quasi-biennial standing wave in the Southern Hemisphere and interrelations with sea surface temperature, Q. J. Roy. Meteorol. Soc., 101, 55–74, doi:10.1002/qj.49710142706, 1975.
Trenberth, K. E.: Fluctuations and trends in indices of the southern hemispheric circulation, Q. J. Roy. Meteorol. Soc., 102, 65–75, 1976.
Urrutia, R. B., Lara, A., Villalba, R., Christie, D. A., Le Quesne, C., and Cuq, A.: Multicentury tree ring reconstruction of annual streamflow for the Maule River watershed in south central Chile, Water Resour. Res., 47, W06527, doi:10.1029/2010WR009562, 2011.
Vautard, R. and Ghil, M.: Singular spectrum analysis in nonlinear dynamics, with applications to paleoclimatic time series, Physica D, 35, 395–424, doi:10.1016/0167-2789(89)90077-8, 1989.
Veblen, T. T.: Regeneration patterns in *Araucaria araucana* forests in Chile, J. Biogeogr., 9, 11–28, 1982.
Veblen, T. T., Kitzberger, T., Raffaele, E., and Lorenz, D. C.: Fire History and Vegetation Changes in Northern Patagonia, Argentina, in: Fire and Climatic Changes in Temperate Ecosystems of the Western Americas, vol. 160, edited by: Veblen, T. T., Baker, W. L., Montenegro, G., and Swetnam, T. W., Springer-Verlag, New York, 265–295, 2003.
Villalba, R. and Veblen, T. T.: Spatial and temporal variation in *Austrocedrus* growth along the forest-steppe ecotone in northern Patagonia, Can. J. Forest. Res., 27, 580–597, 1997.
Villalba, R., Boninsegna, J. A., Lara, A., Veblen, T. T., Roig, F. A., Aravena, J. C., and Ripalta, A.: Interdecadal climatic variations in millennial temperature reconstructions from southern South America, in: Climatic variations and forcing mechanisms of the last 2,000 years, vol. 41, edited by: Jones, P. D., Bradley, R. S., and Jouzel, J., Springer, Berlin, 161–189, 1996.
Villalba, R., Cook, E. R., Jacoby, G. C., D'Arrigo, R., Veblen, T. T., and Jones, P. D.: Tree-ring based reconstruction of northern Patagonia precipitation since AD 1600, Holocene, 8, 659–674, 1998.
Visbeck, M.: A station-based Southern Annular Mode index from 1884 to 2005, J. Climate, 22, 940–950, 2009.
Wigley, T. M. L., Briffa, K., and Jones, P. D.: On the average value of correlated time series, with applications in dendroclimatology and hydrometeorology, J. Clim. Appl. Meteorol., 23, 201–213, 1984.

CPD
7, 3541–3575, 2011

Woodhouse, C. A. and Lukas, J.: Multi-century tree-ring reconstructions of Colorado streamflow for water resource planning, Climatic Change, 78, 293–315, 2006.
Woodhouse, C. A., Gray, S. T., and Meko, D. M.: Updated streamflow reconstructions for the Upper Colorado River Basin, Water Resour. Res., 42, W05415, doi:10.1029/2005WR004455, 2006.

CPD
7, 3541–3575, 2011

Table 1. Descriptive statistics for composite chronologies.

Species/ comp. code	Complete period	Period EPS[1] > 0.85	n. of sites	n. of series	Raw data RW[2] (nm)	Raw data MS[3]	Standard chronology Mean RBAR[4]	Standard chronology Autocorrel.[5]	AR[6] Model	Correl. coeff. with O-J Neuquén River streamflow[7]
					Araucaria araucana					
AR1	1162-2006	1345-2006	11	487	0.854	0.204	0.150	0.671	AR(5)	**0.440**
AR2	1264-2006	1645-2006	3	70	0.859	0.203	0.160	0.759	AR(5)	**0.204**
AR3	1450-2006	1710-2006	2	81	1.016	0.211	0.168	0.649	AR(4)	**0.299**
					Austrocedrus chilensis					
AU1	1461-2003	1486-2003	16	541	0.669	0.266	0.199	0.640	AR(7)	**0.283**
AU2	1144-2005	1200-2005	4	406	0.642	0.263	0.221	0.630	AR(3)	0.104
AU3	1540-2002	1675-2002	4	156	0.895	0.290	0.251	0.595	AR(3)	**0.240**
AU4	955-2002	1160-2002	5	369	0.633	0.257	0.187	0.626	AR(6)	**0.524**
AU5	1613-1975	1670-1975	2	64	0.654	0.215	0.283	0.706	AR(3)	0.075
AU6	190-2005	1125-2005	2	271	0.834	0.264	0.168	0.668	AR(3)	**0.258**

[1] EPS = Expected population signal; [2] RW = Mean ring width; [3] MS = mean sensitivity; Mean RBAR[4] mean correlation between series; [5] Autocorrel. = serial correlation coefficient for the chronology at a lag of 1 year (i.e. the first order autocorrelation); [6] AR(n) = is the autoregressive process of order n used to model the tree-ring series (Cook, 1987) The autocorrelation order n was determined by the minimum Akaike information criterion procedure (Priestley, 1992). [7] Correl. coeff. with O-J Neuquén River streamflow = correlation coefficient between the October–June Neuquén River streamflow and the composite chronologies. Bold numbers indicate significant values at the 0.05 α-level.

Table 2. Calibration and verification statistics for six nested reconstruction models.

Model (period covered by predictors)	Number of variables N_{lc}^1	N_{sc}^2	N_{pp}^3	N_{fp}^4	Calibration period	Verification period	$r_{adj}^{2,5}$	Variance explained (%)	P^6	RE[7]	CE[8]	Sign test
1. 1711–2000	28	11	5	2	1903–2000		0.449	47.2				
					1951–2000	1903–1950	0.472	49.4	0.702	0.283	0.234	40+10-
					1903–1950	1951–2000	0.438	45.0	0.671	0.422	0.353	37 + 11 –
2. 1676–2000	**24**	**10**	**4**	**2**	**1903–2000**		**0.459**	**48.2**				
					1951–2000	**1903–1950**	**0.528**	**55.7**	**0.746**	**0.394**	**0.352**	**42 + 8 –**
					1903–1950	**1951–2000**	**0.438**	**45.0**	**0.671**	**0.422**	**0.353**	**37 + 11 –**
3. 1646–2000	20	9	3	3	1903–2000		0.423	43.5				
					1951–2000	1903–1950	0.521	55.1	0.742	0.402	0.361	42 + 8 –
					1903–1950	1951–2000	0.438	45.0	0.671	0.422	0.353	37 + 11 –
4. 1487–2000	**16**	**8**	**3**	**3**	**1903–2000**		**0.441**	**45.3**				
					1951–2000	**1903–1950**	**0.493**	**51.4**	**0.717**	**0.412**	**0.371**	**41 + 9 –**
					1903–1950	**1951–2000**	**0.438**	**45.0**	**0.671**	**0.422**	**0.353**	**37 + 11 –**
5. 1346-2000	**12**	**5**	**2**	**2**	**1903–2000**		**0.419**	**43.1**				
					1951–2000	**1903–1950**	**0.468**	**49.0**	**0.700**	**0.393**	**0.351**	**39 + 11 –**
					1903–1950	**1951–2000**	**0.368**	**38.2**	**0.618**	**0.383**	**0.309**	**36 + 12 –**
6. 1161–2000	8	4	2	2	1903–2000		0.307	32.2				
					1951–2000	1903–1950	0.406	43.0	0.656	0.22	0.160	35 + 13 –
					1903–1950	1951–2000	0.289	30.4	0.551	0.066	−0.046	35 + 13 –

[1] N_{lc} = number of lagged composite chronologies, [2] N_{sc} = number lagged composite chronologies significantly correlated with the streamflow record, [3] N_{pp} = number of PCs in pool of potential predictors, [4] N_{fp} = and number of PCs included as predictors in final model, [5] r_{adj}^2 = the square of the multiple correlation coefficient adjusted for loss of degrees of freedom, [6] P = Pearson's correlation coefficient, Sign Test results for calibration period indicate number of years in which tree-ring estimates correctly, + (incorrectly, –) track sign of observations (Cook et al., 1990). Verification: [7] RE = reduction of error, [8] CE = coefficient of efficiency statistics.

Table 3. Lowest and highest n year moving averages of the reconstructed (1346–2000) and measured streamflow (1903–2009). Events are non-overlapping averages of the mean October–June Neuquén River streamflow ($m^3 s^{-1}$) for n year periods. Ranks 1–5 are the most severe reconstructed events and actual is the most severe observed event.

Rank	Droughts				Pluvials			
	1 Year	5 year	10 year	25 year	1 Year	5 year	10 year	25 year
1	43.7 (1968)	161.3 (1817–1821)	188.8 (1908–1917)	236.2 (1802–1826)	619.9 (1589)	456.2 (1589–1593)	421.4 (1829–1838)	385.5 (1349–1373)
2	64.1 (1998)	161.7 (1909–1913)	193.3 (1812–1821)	237.5 (1889–1913)	570.3 (1940)	446.1 (1833–1837)	419.9 (1584–1593)	378.4 (1927–1951)
3	74.2 (1819)	167.9 (1889–1893)	194.9 (1888–1897)	264.8 (1952–1976)	560.8 (1635)	442.7 (1357–1361)	414.5 (1359–1368)	356.6 (1465–1489)
4	75.7 (1924)	171.6 (1966–1970)	226.5 (1858–1867)	270.4 (1765–1789)	556.7 (1992)	438.2 (1929–1933)	407.0 (1932–1941)	356.0 (1828–1852)
5	79.2 (1813)	177.7 (1958–1962)	229.6 (1953–1962)	271.0 (1677–1701)	540.9 (1634)	435.5 (1938–1942)	397.3 (1634–1643)	355.1 (1582–1606)
Actual	78.1 (1998)	186.7 (1995–1999)	242.9 (1990–1999)	277.9 (1975–1999)	627.3 (1914)	413.0 (1930–1934)	402.2 (1930–1939)	350.3 (1925–1949)

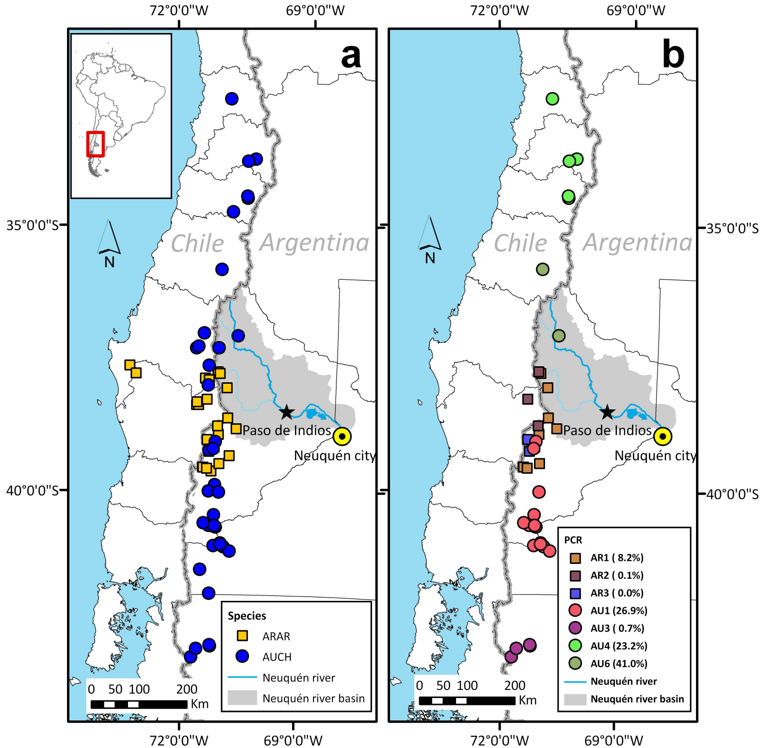

Fig. 1. Maps showing the Neuquén River basin (shaded area), the location of the Paso de Indios gauging station (black star), and the location of the 66 tree-ring sites initially considered as predictors **(a)** and the final subset of chronologies **(b)** in the reconstruction. Sites are differentiated by species in **(a)** and by beta weights of the composite chronologies over their common period 1676–2000 AD **(b)**. The beta weights represent the explanatory power of the composite chronologies (see text for details). ARAR: *Araucaria araucana*; AUCH: *Austrocedrus chilensis*. For composite chronologies codes, see Table 1 in the Supplement.

CPD
7, 3541–3575, 2011

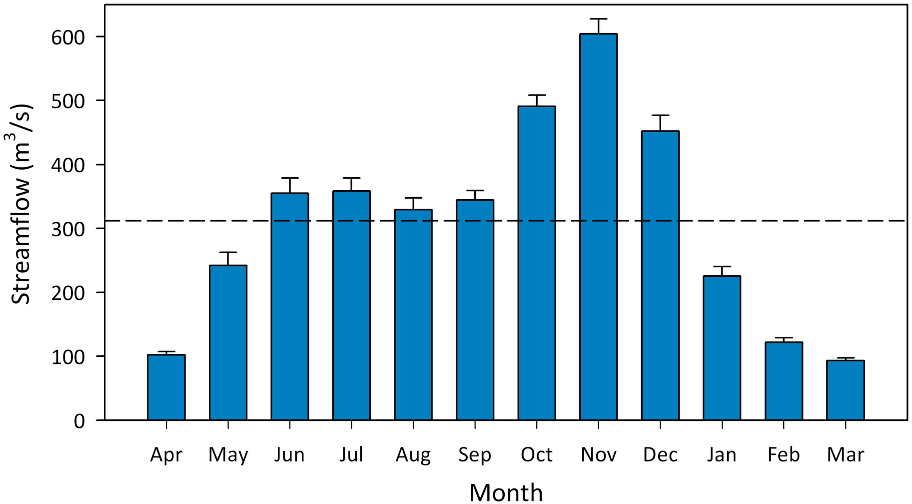

Fig. 2. Mean monthly variations of the Neuquén River streamflow at the Punta de Indios gauging station (period 1903–2009) over the complete hydrological year (April–March). Dashed line represents the historical mean (312 $m^3 s^{-1}$) for the 1903–2009 period.

Discussion Paper | Discussion Paper | Discussion Paper | Discussion Paper |

CPD
7, 3541–3575, 2011

Title Page
Abstract | Introduction
Conclusions | References
Tables | Figures
◀| |▶
◀ ▶
Back | Close
Full Screen / Esc
Printer-friendly Version
Interactive Discussion

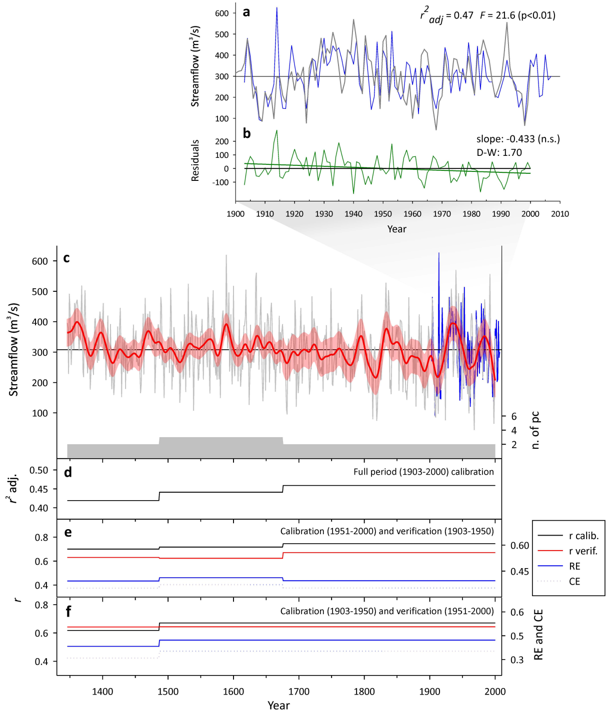

Fig. 3. October–June Neuquén River streamflow reconstruction for the past 655 years. **(a)** Instrumental (blue) and nested tree-ring reconstructed (gray) streamflow for the 1903–2000 common period. The coefficient of determination (an indicator of the proportion of variance explained by regression) adjusted for the degrees of freedom in the model (r^2_{adj}), the F-value of regression (the ratio between the explained and the explained variability in the model) for Model 2 are also shown. Regression residuals for the reconstruction are shown in **(b)**. The linear trend of regression residuals (slope) and the Durbin-Watson (D-W) statistics used to test for first-order autocorrelation of the regression residuals are also indicated. **(c)** Nested tree-ring based reconstruction of the October–June Neuquén River streamflow for the period 1346–2000. The thick red line represents a 25-yr cubic spline to emphasize the long-term variations in the Neuquén River streamflow reconstruction. Red shading represents the ±2 RMSE uncertainty bands in this smoothed series. Gray shading reflects the number of predictors available over time. **(d)** Variations in the adjusted coefficient of determination (r^2_{adj}) for the full period calibration. **(e)** and **(f)** Pearson correlation coefficient (r), the reduction of error (RE), the coefficient of efficiency (CE) for the split calibration and verification periods.

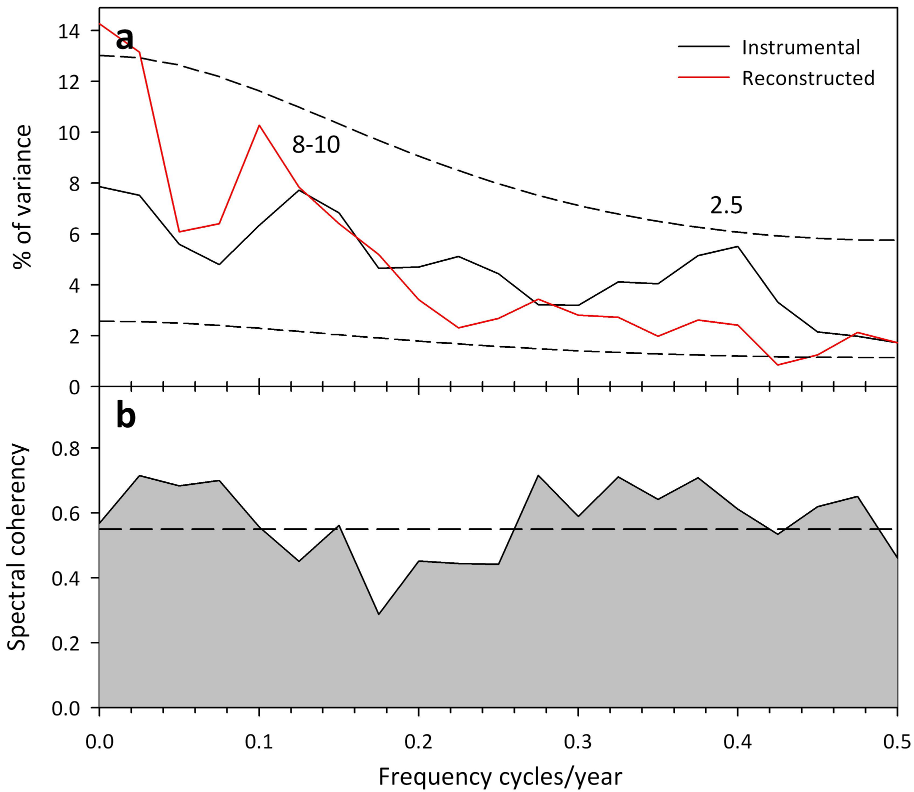

Fig. 4. Blackman-Tukey **(a)** and coherency **(b)** spectra of actual and reconstructed Neuquén River streamflow over the period 1903–2000. In both panels, dashed lines represent the 95 % confidence limits. For the Blackman Tukey spectra the 95 % confidence limits are shown for instrumental streamflow records. The 95 % confidence limits are based on a 1st-order Markov null continuum model. The periods are given in years for most prominent peaks.

CPD
7, 3541–3575, 2011

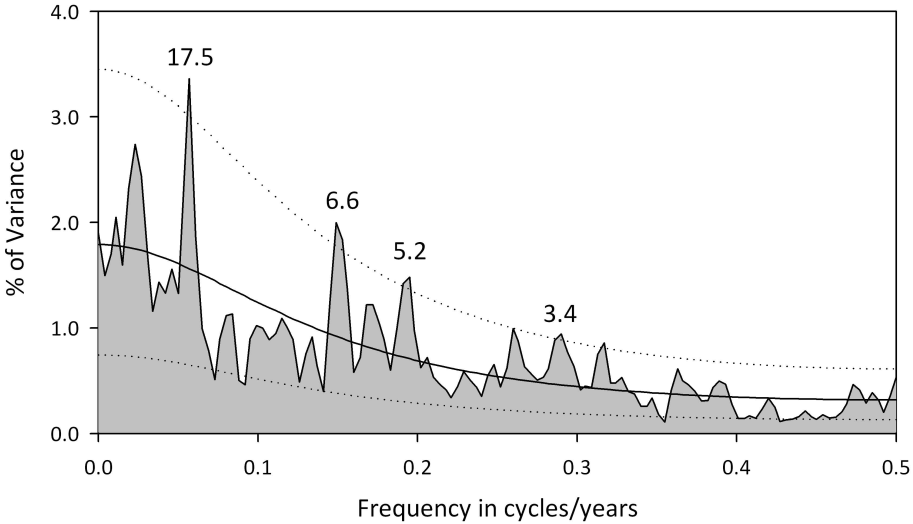

Fig. 5. The Blackman-Tukey spectral density of the reconstructed Neuquén River streamflow (1346–2000). The dotted lines represent the 95 % confidence interval and the dashed line is the red noise band.

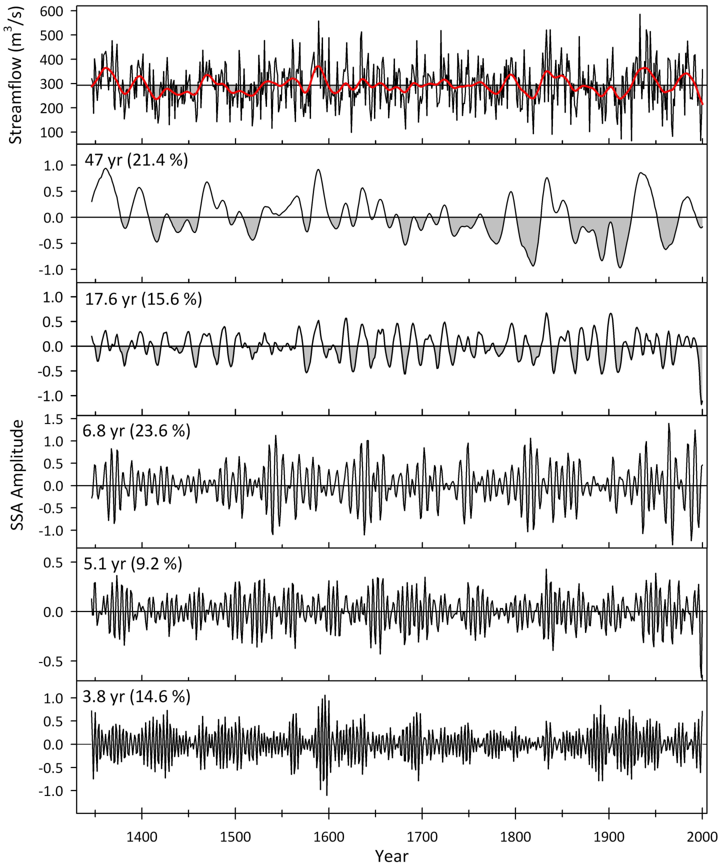

Fig. 6. The Neuquén River streamflow reconstruction (top panel) and its most significant oscillation modes estimated using singular spectrum analysis (SSA). Units are dimensionless. Periods in years and the percentage of variance associated with each waveform are shown in the upper-left corners of the streamflow waveforms.

CPD
7, 3541–3575, 2011

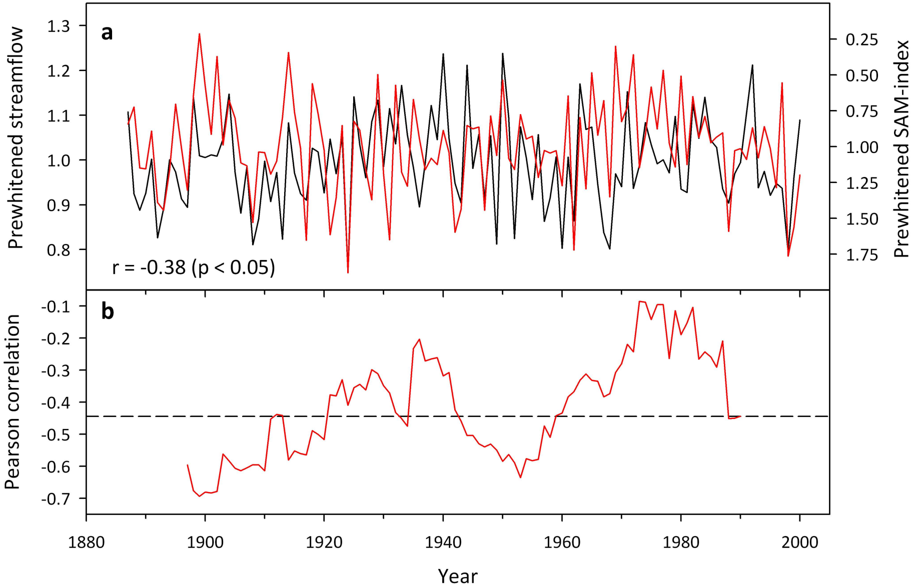

Fig. 7. (a) Relationship between the October–June Neuquén River streamflow and annual SAM index for the period 1887–2000. SAM index has been inverted to facilitate the comparison with the streamflow data. **(b)** 21-year central moving correlations between the streamflow and the annual SAM index. Dashed line indicates the 0.05 significance level. Note the change in strength of this relationship over time.

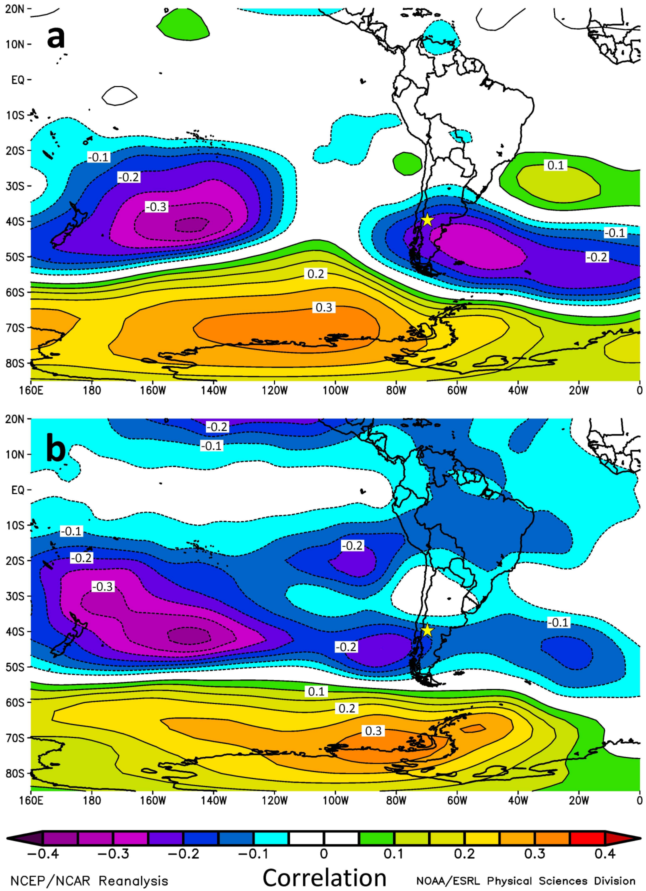

Fig. 8. Spatial correlation patterns during the interval 1948–2000 between October–June 500 HPa geopotential height anomalies and **(a)** instrumental and **(b)** reconstructed October–June Neuquén River streamflow. The yellow stars indicate the location of Paso de Indios gauging station. Solid and dashed contours indicate positive and negative correlations, respectively; zero contours are omitted. Correlation analyses and gridded geopotential height data were obtained from the National Oceanic and Atmospheric Administration website (http://www.esrl.noaa.gov/psd/data/correlation/).

CPD
7, 3541–3575, 2011